Structural and functional studies of a *Fusarium oxysporum* cutinase with polyethylene terephthalate modification potential

Maria Dimarogona, Efstratios Nikolaivits, Maria Kanelli, Paul Christakopoulos, Mats Sandgren, Evangelos Topakas

PII: S0304-4165(15)00218-4
DOI: doi: 10.1016/j.bbagen.2015.08.009
Reference: BBAGEN 28260

To appear in: *BBA - General Subjects*

Received date: 10 May 2015
Revised date: 9 August 2015
Accepted date: 14 August 2015

Please cite this article as: Maria Dimarogona, Efstratios Nikolaivits, Maria Kanelli, Paul Christakopoulos, Mats Sandgren, Evangelos Topakas, Structural and functional studies of a *Fusarium oxysporum* cutinase with polyethylene terephthalate modification potential, *BBA - General Subjects* (2015), doi: 10.1016/j.bbagen.2015.08.009

Structural and functional studies of a *Fusarium oxysporum* cutinase with polyethylene terephthalate modification potential

Maria Dimarogona[1,3], Efstratios Nikolaivits[1], Maria Kanelli[1], Paul Christakopoulos[2], Mats Sandgren[3], Evangelos Topakas[1*]

[1]*Biotechnology Laboratory, School of Chemical Engineering, National Technical University of Athens, 5 Iroon Polytechniou Str., Zografou Campus, Athens 15780, Greece*

[2]*Biochemical and Chemical Process Engineering, Division of Sustainable Process Engineering, Department of Civil, Environmental and Natural Resources Engineering, Luleå University of Technology, SE-97187 Luleå, Sweden*

[3]*Department of Chemistry and Biotechnology, Swedish University of Agricultural Science, SE-75007, Uppsala, Sweden*

[*]Correspondence to: E. Topakas. Tel: +30-210-7723264; fax: +30-210-7723163; e-mail: vtopakas@chemeng.ntua.gr

ABSTRACT

Background: Cutinases are serine hydrolases that degrade cutin, a polyester of fatty acids that is the main component of plant cuticle. These biocatalysts have recently attracted increased biotechnological interest due to their potential to modify and degrade polyethylene terephthalate (PET), as well as other synthetic polymers.

Methods: A cutinase from the mesophilic fungus *Fusarium oxysporum*, named *Fo*Cut5a, was expressed either in the cytoplasm or periplasm of *Escherichia coli* BL21. Its X-ray structure was determined to 1.9 Å resolution using molecular replacement. The activity of the recombinant enzyme was tested on a variety of synthetic esters and polyester analogues.

Results: The highest production of recombinant *Fo*Cut5a was achieved using periplasmic expression at 16^{o}C. Its crystal structure is highly similar to previously determined *Fusarium solani* cutinase structure. However, a more detailed comparison of the surface properties and amino acid interactions revealed differences with potential impact on the biochemical properties of the two enzymes. *Fo*Cut5a showed maximum activity at 40^{o}C and pH 8.0, while it was active on three *p*-nitrophenyl synthetic esters of aliphatic acids (C_2, C_4, C_{12}), with the highest catalytic efficiency for the hydrolysis of the butyl ester. The recombinant cutinase was also found capable of hydrolyzing PET model substrates and synthetic polymers.

Conclusions: The first reported expression and crystal structure determination of a functional cutinase from the mesophilic fungus *F. oxysporum* with potential application in surface modification of PET synthetic polymers.

General significance: *Fo*Cut5a could be used as a biocatalyst in industrial applications for the environmentally-friendly treatment of synthetic polymers.

Keywords: heterologous expression; *Escherichia coli*; serine esterase; PET modification; crystal structure

1 INTRODUCTION

Cutin is one of the two main constituents of the plant cuticle, the first barrier of plants against invading pathogens. Although its exact structure and composition varies among plants, organs and growth stages, cutin is an insoluble lipid polymeric network made of oxygenated C_{16} and C_{18} fatty acids linked by ester bonds [1]. Cutinases (E.C 3.1.1.74) are extracellular serine esterases employed by most phytopathogens and saprophytes in order to degrade cutin [2]. They are divided into three subfamilies, two fungal and one bacterial, based on phylogenetic analysis [3]. Even though all cutinases display similar catalytic profiles, there is substantial difference in terms of primary structure between eukaryotic and prokaryotic enzymes [4]. Up to now, X-ray structures of six fungal and two bacterial cutinases have been solved and they shed light on the structure-function relations of these particular biocatalysts. They all have an α/β fold, with an active site consisting of a catalytic triad composed of a serine, a histidine and an aspartic acid [5]. The catalytic serine is exposed to the solvent and there is no lid above the active site as found in the case of the lipases [6]. Cutinases are capable of hydrolyzing *p*-nitrophenyl esters ranging from C_4 to C_{18}, with butyrate (C_4) being the preferred substrate for the majority of them. These enzymes can also degrade high molecular weight polyesters, artificial triglycerides and perform esterification and transesterification reactions without displaying interfacial activation, which occurs in the case of lipases [6].

These biocatalysts are thus categorized between pure lipases and esterases, and since the discovery of this versatile activity, intensive research efforts have been focused on the use of cutinases in a number of industrial applications [7]. Currently, this class of enzymes is widely used within textile industry, for the removal of wax particles from cotton and the surface modification of synthetic fibers [8]. Enzymatic treatment of polyethylene terephthalate (PET) used for modification of clothing fibers aims at altering their surface properties such as hydrophobicity, reducing bacterial adhesion, and improving dying capacity while maintaining bulk characteristics of the fiber. In addition to the surface modification, cutinases can be used for PET degradation, since the chemical procedure requires harsh conditions and is uneconomical and environmentally non-friendly [9].

In the present study, we set out to biochemically and structurally characterize a cutinase from the mesophilic fungus *Fusarium oxysporum* (*Fo*Cut5a). This enzyme is

highly homologous to the well-characterized cutinase from *F. solani pisi* [5, 10], which has been efficiently used in a wide range of biocatalytic applications, including PET modification [10-12]. Interestingly, a recent work showed that a crude cutinase preparation from a newly isolated *F. oxysporum* strain (LCH1) could hydrolyze PET more efficiently than the *F. solani* enzyme, indicating the potential use of *F. oxysporum* as a source of efficient novel biocatalysts [13]. *Fo*Cut5a cDNA gene, constructed by Overlap Extension Polymerase Chain Reaction (OEPCR), was cloned and expressed in *Escherichia coli* BL21. The recombinant protein was purified, crystallized and its three-dimensional structure was determined by X-ray crystallography. The expressed *Fo*Cut5a protein was biochemically characterized based on the substrate specificity and ability to hydrolyze PET model substrates and synthetic polymers, indicating its potential use in biotechnological applications.

2 MATERIALS AND METHODS

2.1 Chemicals and enzymes

VentR® DNA and KOD Hot Start polymerases were purchased from New England Biolabs (UK) and Novagen (USA), while restriction enzymes were purchased from TAKARA (Japan). NucleoSpin® Gel-PCR Clean-up and GenElute™ Plasmid Miniprep were purchased from Macherey Nagel (Germany), and Sigma-Aldrich (USA), respectively. Three *p*-nitrophenyl monomer esters, *p*-nitrophenyl acetate (*p*NPhA), *p*-nitrophenyl butyrate (*p*NPhB) and *p*-nitrophenyl laurate (*p*NPhL), as well as bis(2-hydroxyethyl) terephthalate (BHET) and polycaprolactone (PCL), were purchased from Sigma-Aldrich. Commercial PET woven fabric with tricot knit was kindly supplied by Colora S.A (Greece). Trifluoroacetic acid and acetonitrile were of HPLC (High Performance Liquid Chromatography) grade (Sigma-Aldrich). All other reagents and organic solvents used were of analytical grade.

2.2 Strains, vectors and media

For the cloning of cutinase gene from *F. oxysporum (cut5a), E. coli* One Shot® Top10 and Zero Blunt® PCR Cloning Kit (Invitrogen, USA) were used as the host-vector system. The bacterial strain *E. coli* BL21 (DE3) and vector pET-22b(+) (Novagen, USA) were used for protein expression. The wild type strain of *F. oxysporum*

PHW815 (NRRL54008), was maintained on potato–dextrose–agar (PDA) at 4 ^{o}C and its total genomic DNA was isolated, as described previously [14]. *E. coli* BL21 was grown at 37 ^{o}C in Luria-Bertani (LB) medium containing 50 μg kanamycin mL^{-1} for selection of clones transformed with the Zero Blunt® PCR vector and 100 μg ampicillin mL^{-1} for selection of clones transformed with pET-22b(+) vector.

2.3 Cloning of cutinase gene and cDNA synthesis by OEPCR

The gene coding for the hypothetical protein *Fo*Cut5a (*cut5a*) was PCR amplified from genomic DNA using primers designed based upon the available *foqg_13916.1* gene sequence (*F. oxysporum* Sequencing Project. Broad Institute of Harvard and MIT;http://www.broadinstitute.org/annotation/genome/fusarium_group/MultiHome.html), including the *Nde*I and *Not*I restriction enzyme sites at their respective 5'-ends (*Fo*Cut5a_F and *Fo*Cut5a_R, Table 1). A high fidelity VentR® DNA polymerase producing blunt ends was used for the DNA amplification which was carried out with 40 cycles of denaturation (20 s at 95^{o}C), annealing (10 s at 55^{o}C), and extension (20 s at 70^{o}C), followed by 5 min of further extension at 70^{o}C. In order to determine the DNA sequence, PCR products were directionally cloned into the pCR-Blunt® vector by standard procedures described by the Zero Blunt® PCR Cloning Kit. Intron removal was achieved by using the molecular technique of OEPCR. Two complementary DNA primers, two external primers (Table 1), and the appropriate PCR amplification process were used to generate two DNA fragments having overlapping ends. The recombinant plasmid pCR-Blunt/*cut5a*, at an appropriate dilution, was used as template DNA, while the reaction catalysis was held by VentR® DNA polymerase. The PCR conditions for each reaction programmed for optimal product amplification are given as following: for the first exon, (primers *Fo*Cut5a_F and *Fo*Cut5a_eR), 95 °C for 2 min, followed by 40 cycles of 95 °C for 20 s, 55 °C for 10 s and 70 °C for 20 s, with a final extension step at 70 °C for 2 min. For the second exon, (primers *Fo*Cut5a_eF and *Fo*Cut5a_R), 95 °C for 2 min, followed by 40 cycles of 95 °C for 20 s, 57 °C for 10 s and 70 °C for 40 s, with a final extension step at 70 °C for 2 min.

The resulting two PCR products were combined together in a subsequent hybridization reaction resulting in a heteroduplex structure, in which the overlapping ends annealed in a complementary fashion, allowing the 3′ overlap of each strand to

serve as a primer for the 3′ extension of the complementary strand. The generated "fusion" fragment was amplified further by a PCR, through the utilization of the two external primers, *Fo*Cut5a-F and *Fo*Cut5a-R, with an initial denaturation step at 95 °C for 2 min, followed by 35 cycles at 95 °C for 20 s, 57 °C for 10 s, 70 °C for 30 s and a final extension step at 70 °C for 1 min. The final PCR product was cloned into the pCR-Blunt® vector after PCR-clean up using Nucleospin kit (Macherey-Nagel, Germany) and further verified by DNA sequencing analysis of both strands.

For the introduction of pelB coding sequence embedded in pET-22b(+) vector, resulting in periplasmic expression, the introduction of a *Nco*I restriction site was performed. Using as template the recombinant pCR-Blunt® already constructed and primers *Fo*Cut5a-pelBF and *Fo*Cut5a-R, the PCR was initiated with a denaturation step at 95 °C for 2 min and thereafter an additional 35 cycles of 95 °C for 20 s, 57 °C for 20 s, 70 °C for 30 s and a final extension step at 70 °C for 1 min. The reaction product was cloned into the pCR-Blunt® vector. Both constructs were cloned in the pET-22b(+) expression vector after amplification and digestion in the pCR-Blunt® plasmid.

2.4 Heterologous expression and purification of *Fo*Cut5a

The recombinant expression plasmids were used to transform chemically competent *E. coli* BL21 (DE3). The transformants were cultured in LB-ampicillin broth at 37 ^{o}C to mid-exponential phase (OD600 of approx. 0.6-1.0) and recombinant protein expression was induced by the addition of 1 m*M* isopropyl 1-thio-β-D-galactopyranoside (IPTG) and further incubation for 20 h at 37 ^{o}C or 16 ^{o}C. After induction, the cultures were centrifuged at 4,000 x *g* for 15 min at 4^{o}C.

Cultures aimed at detecting recombinant cutinase for each expression strategy were performed in 100 mL flasks containing 40 mL LB medium and after centrifugation the supernatant was not concentrated any further. For the purification of *Fo*Cut5a, the supernatant (200 mL) was collected and concentrated using an Amicon ultrafiltration apparatus (exclusion size 10 kDa; Amicon chamber 8400 with membrane Diaflo PM-10, Millipore, USA) that was considered as the extracellular fraction. The centrifuged cells were resuspended in 40 mL of 50 m*M* Tris-HCl buffer containing 300 m*M* NaCl (pH 8.0), and disrupted using the ultrasonic processor VC 600 (Sonics and Materials, USA) applying 5 cycles of 60 s sonication (50% Duty Cycle), at 70% amplitude.

After centrifugation at 10,000 x *g* for 20 min at 4 ^{o}C, the supernatant (cell-free extract) was filtered through 0.45 μm filters. Inclusion bodies isolation and refolding was performed by a modified protocol, as described previously [15]. Both intra- and extracellular fractions were subsequently loaded onto an immobilized metal-ion affinity chromatography (IMAC) column (Talon, Clontech; 1.0 cm i.d., 15 cm length) equilibrated with the same buffer. The column was first washed with 70 mL buffer, then a linear gradient from 0 to 100 m*M* imidazole in 20 m*M* Tris-HCl buffer containing 300 m*M* NaCl (60 mL, pH 8.0) was applied at a flow rate of 2 mL min^{-1}. The purity of isolated *Fo*Cut5a was checked by sodium dodecyl sulphate-polyacrylamide gel electrophoresis (SDS-PAGE) according to the method of Laemmli (1970) [16], using a 12.5% polyacrylamide gel. The isoelectric point (p*I*) of the expressed protein was determined by PhastGel IEF – 3-9 electrophoresis (GE Healthcare Life Sciences).

2.5 Enzyme characterization

Cutinase activity was assayed using *p*NPhB (0.96 m*M*) as substrate in 0.1 *M* citrate phosphate buffer (pH 6.0) at 40 ^{o}C for 10 min, monitoring the release of *p*NPh at 410 nm. One unit of enzyme activity is defined as the amount of enzyme releasing 1 μmol of *p*NPh per minute.

Kinetic studies of the purified enzyme were performed with *p*NPhA, *p*NPhB and *p*NPhL. Kinetic constants (k_{cat}, K_m) were estimated using a non-linear regression model in GraphPad Prism 5 from GraphPad Software that also gives an estimate of the standard error of each parameter.

The optimum temperature was determined by assaying the enzyme activity at various temperatures ranging from 25 to 70 ^{o}C, in 0.1 *M* citrate phosphate buffer, pH 6.0. The thermostability of the expressed protein was determined by measuring the residual activity under standard assay conditions, after incubation of *Fo*Cut5a at temperatures ranging from 20 to 40 ^{o}C for 1 – 3 h in the absence or presence of calcium cations (100 m*M* $CaCl_2$). The optimum pH was determined by assaying the enzyme activity in various buffers in the pH range 3.0 to 9.0, using the following buffers: 0.1 *M* citrate-phosphate (pH 3.0-7.0), 0.1 *M* Tris-HCl (pH 8.0-9.0).

Protein concentration for purified enzymes was determined by measuring A_{280} [17] using a calculated molar extinction coefficient of 16180 M^{-1} cm^{-1}.

2.6 Crystallization and structure determination

Purified *Fo*Cut5a was concentrated to 10 mg/ml in 20 m*M* Tris HCl pH 8 and submitted to a high-throughput crystallization screening using a Mosquito crystallization robot (TTP Labtech, UK) and commercially available 96-well kits (JCSG+ and Morpheus HT (Molecular Dimensions), PACT (Qiagen), PEG/ION and INDEX HT (Hampton Research)). Diffracting plate-like crystals grew after a couple of days at room temperature in the presence of 12.5% PEG3350, 12.5% 2-Methyl-2,4-pentadiol (MPD) and 12.5% PEG 1000. X-ray diffraction data were collected on a single crystal to 1.9 Å resolution on beamline ID23-2 (ESRF, France) under cryogenic conditions. The wavelength of the X-ray beam was 0.8726 Å, and the oscillation range 0.1^{o}. The resulting dataset was processed using XDS [18] and structure was solved by molecular replacement using PHASER [19]. The molecular replacement search model was produced using CHAINSAW [20] and *Fusarium solani* cutinase as the template structure (PDB ID: 1CEX) [21] (80% sequence identity for 90% sequence coverage). Iterative rounds of model building and refinement of the structure were performed using COOT [22] and REFMAC from the CCP4i program suite [23]. Solvent molecules were added using COOT, and checked manually. The quality of the final structure model was evaluated using MOLPROBITY [24]. The final structure model and the structure factors are deposited at the PDB under accession code 5AJH. Data collection and refinement statistics are summarized in Table 2. All structure figures were prepared using UCSF Chimera package [25] .

2.7 Enzymatic hydrolysis of PET model substrates, PET fabrics and PCL

The synthesis of the PET model substrate bis-benzoyloxyethyl terephthalate (3PET) was carried out using benzoylchloride, 2-chloroethanol for the synthesis of the intermediate benzoic acid 2-chloroethylester, while dimethylformamide, triethylamine (Sigma, USA) and terephthalic acid (TA) (Merck, USA) were used subsequently for the production of the final compound, as previously described [26]. 3PET was purified by flash column chromatography on silica gel 60 (Merck), using toluene/ethyl acetate (5:1, v/v) and identified with a Bruker DRX 400 NMR spectrometer, equipped with a 5 mm $^{1}H/^{13}C$ dual inverse broad probe operating at 400 MHz.

*Fo*Cut5a catalytic activity experiments, using either 3PET or commercially available BHET as substrates, were performed by incubating 2 or 10 mg of each compound, respectively, with 0.07 mg enzyme in 1 mL of 100 m*M* Tris-HCl pH 7, at 30 ^{o}C for 18 h. Prior to HPLC analysis, the reactions were terminated by adding 20 µL concentrated sulphuric acid and thereafter filtered to obtain a clean soluble fraction of the hydrolysis reaction [26]. The samples were analyzed by HPLC, using a SHIMADZU LC-20AD equipped with a Jasco UV-975 detector recording at 241 nm. The reversed phase column Eurospher-100 C18 from KNAUER (Germany) was maintained at room temperature. A linear gradient method, involving 1% trifluoroacetic acid solution and acetonitrile as eluents at a flow rate of 0.8 mL/min, was applied as previously described [11].

PET polyester hydrolysis leads to the release of TA, MHET and BHET among other esterified oligomers with higher MW. TA and its derivatives show a maximum absorption in the range of 240-244 nm [27]. Therefore, a calibration curve of TA was used for the quantification of total TA and TA derivatives released as equivalents, by measuring the absorbance of the supernatant at 241 nm in a BOECO S-20 Spectrophotometer (Germany), as previously reported [11]. Appropriate control reactions without polyester were carried out to subtract the protein absorbance at 241 nm. For the surface modification of PET fabrics, 1 g polyester was incubated in glass vessels at a bath ratio of 1:50 (textile mass over buffer mass), under stirring (170 rpm) and at an enzyme concentration of 0.94 mg/g fabric, at 30 ^{o}C, in 100 mM phosphate buffer pH 7, for 24 h.

For the enzymatic hydrolysis of polyester PCL, 0.07 mg of *Fo*Cut5a was mixed with 20 mg PCL in 1 mL of 100 m*M* Tris-HCl pH 7 and incubated at 40 ^{o}C for 18 h. The degree of hydrolysis was estimated by calculating the weight loss of the samples after drying, as previously described [28]. All measurements were performed in duplicate.

3 RESULTS AND DISCUSSION

3.1 Identification of *Fo*Cut5a as a putative cutinase

Fusarium species represent excellent model organisms to study the infection process in soilborne and leaf fungal pathogens. The pea pathogen *F. solani* f.sp. *pisi* attacks the aerial parts of plants by secreting cutinases that facilitate penetration of the outermost cuticular barrier of the host [29]. Its genome encodes three putative cutinases: *cut1*, which is induced in the presence of cutin monomers, and *cut2* and

cut3 that are expressed constitutively in low amounts [30]. The role of cutinases in plant infection by pathogens that attack the cuticle-less roots, such as *F. oxysporum* is still poorly understood. Numerous attempts to isolate *F. oxysporum* cutinase genes, using primers derived from conserved regions of *F. solani* cutinase genes yielded the same amplified fragment, underpinning the presence of a single gene encoding this family of cutinases in the genome of *F. oxysporum* [31]. This is in accordance to the annotated *F. oxysporum* genomic database (http://www.broadinstitute.org), as well as to the Carbohydrate-Active enZymes (CAZy) database http://www.cazy.org/. [32] The different number of cutinase genes in the two *Fusarium* species could be explained by a divergent evolutionary mechanism during adaptation of the infection process in root and aerial plant pathogens [31].

The open reading frame (ORF) of *cut5a*, found in *foqg_13916.1* accession of *F. oxysporum* genomic database, encodes a protein of 230 amino acids including a secretion signal peptide of 16 amino acids (MKFSIISTLLAATASA), predicted by SignalP (http://www.cbs.dtu.dk/services/SignalP). A search using the BLAST program at NCBI [33] showed that *Fo*Cut5a exhibits the highest sequence identity with already characterized cutinases, such as e.g. the three cutinases from *F. solani* (ranging from 76 to 78 %) [31], a cutinase from *Colletotrichum gloeosporioides* (51%) [34] and a cutinase from *Aspergillus oryzae* (47%) [28] (Fig. S1). The predicted mass and p*I* of the mature protein were 21739 Da and 8.37, respectively, by calculations using the ProtParam tool of ExPASY (http://au.expasy.org/tools/protparam.html). The translated sequence of *cut5a* gene does not present any potential *N*-glycosylation sites, as predicted by using the NetNGlyc 1.0 server (http://www.cbs.dtu.dk/services/NetNGlyc/) [35]. As there is no need for post-translational *N*-glycosylation, the heterologous expression in a prokaryote host, such as *E. coli*, was used, resulting in a functional soluble recombinant biocatalyst.

3.2 Heterologous expression of recombinant cutinase

Expression of eukaryotic proteins that contain cysteine residues, in *E. coli*, can be challenging, due to wrong post-translational processing. Cytoplasm is a reducing environment where disulphide bonds may or may not be formed. The structure of *F. solani* cutinase (PDB ID: 1CEX), which is highly homologous *Fo*Cut5a, indicated the

presence of two disulfide bridges, potentially contributing to the structural integrity of the secreted enzyme. This suggested the need for expressing the recombinant enzyme in the oxidizing environment of the bacterial periplasm. Further enhancement in protein expression was attempted by testing different induction temperatures.

Expression in the cell cytoplasm resulted in the intracellular localization of the recombinant protein, which in case of induction at 37 ^{o}C was detected almost completely (98.5%) as inclusion bodies, while at 16 ^{o}C as soluble protein. In both cases only traces of cutinase activity were detected in the culture medium (approximately 1% of full activity). The highest protein expression yield was achieved utilizing periplasmic expression of the cutinase at low temperature (16 ^{o}C), reaching 3960 U of total activity, which originated from 40 ml of starting culture. Cutinase activity was distributed in three fractions, including the extracellular liquid (41% of total activity), cell free extract (54% of total activity) and inclusion bodies. When the temperature was increased to 37 ^{o}C, the total amount of produced enzyme was reduced to 258 U with a large portion leaking in culture supernatant (64 %) and a relatively high amount of inclusion bodies that held the 34 % of total activity. The detection of cutinase activity in the culture supernatant at both induction temperatures, is in accordance with other recently reported studies. In specific, the work by Sulaiman et al. showed that more than 50% of a cutinase cloned from a leaf-branch compost metagenome library and expressed with the signal peptide pelB in *E. coli* BL21-CodonPlus-RP cells, was secreted in the culture medium [36]. Two *Thermobifida fusca* cutinases, Tfu_0882 and Tfu_0883, expressed in *E. coli* BL21-Rosetta reached extracellular productions of 69 and 180 U/mL, respectively [4]. It was further shown that Tfu_0883 "leaked" in the culture medium even without the mediation of pelB signal sequence, due to the hydrolytic activity of the enzyme towards phospholipids, which are an important component of the cell membrane [37].

The recombinant cutinase that was expressed in the periplasmic space of *E. coli* BL21 at 16 ^{o}C, was purified by IMAC and its homogeneity was confirmed by SDS-PAGE where it appeared as a single band (ca. 23 kDa; Fig. 1A). Cutinases are small proteins with molecular weights (MW) of approximately 25 kDa. Closer to the MW of *Fo*Cut5a are the MW of the cutinases from *Thielavia terrestris* (23 kDa) [38], *F. solani* and *Monilinia fructicola* (22 kDa) [39, 40], *Fusarium roseum* and *Colletotrichum capsici* (24 kDa) [34, 41]. Cutinases with higher MW (ca. 30 kDa) are also commonly found among cutinases from fungi (*Trichoderma harzianum*, *A. niger*

and *A. nidulans*), [42-44] and from bacteria (three *Thermobifida* strains) [45-47]. Furthermore, the p*I* of *Fo*Cut5a was determined to be approximately 7.9 (Fig. 1B), which is in accordance to the theoretical p*I* of the protein (8.37). p*I* values of characterized cutinases range between pH 7.5-9.0 [40, 48], while for the *F. solani* cutinase p*I* was estimated to be 7.6 [49].

3.3 Crystal structure of *Fo*Cut5a

*Fo*Cut5a structure was determined at 1.9 Å resolution using the molecular replacement method. The initial search model was derived from *F. solani pisi* cutinase structure, which is a very close homologue, with 80% sequence identity for 90% sequence coverage (Fig. 2). *Fo*Cut5a crystallized in space group $P2_12_12_1$ with 3 molecules in the asymmetric unit. The final model of *Fo*Cut5a has been refined to R_{work}/R_{free} (%) values of 18.1/22.4 for 121-1.9 Å data (Table 2).

In all three non crystallographically related protein molecules found in the asymmetric unit of the protein crystal, there is no electron density for the first 17 N-terminal amino acids of the mature protein, a feature also observed in *F. solani* structure. The fact that these amino acids belong to a pro- peptide which is not present in the mature protein but is required for proper expression, could probably reflect an increased flexibility in this region of the protein and might provide an explanation for the absence of sufficient electron density for modelling this region in both structures [5]. The C-termini of monomers A and B include 4 and 2 additional alanine residues, respectively, derived from the cloning strategy employed for the expression of the recombinant enzyme. In case of poorly defined electron density, observed on the side chains of certain solvent exposed residues, the corresponding atoms were not included in the final refined model.

*Fo*Cut5a displays a typical α/β fold, with a central beta-sheet of 5 parallel strands (β1:Val35-Ala40, β2:Val69-Gly73, β3:Val114-Tyr120, β4:Ile142-Phe148 and β5:Thr168-Phe171), surrounded by 11 helices (α1:Ser29-Ser31, α2:Gly53-Tyr64, α3: Leu82-Ala86, α4:Ser93-Lys109, α5:Gln122-Asp133, α6:Ala136-Lys141, α7:Glu165-Arg167, α8:Leu177-Thr180, α9:Ala187-Leu190, α10:Gln193-Ser197 and α11: Ala199-Ala217). There are two disulphide bridges in each *Fo*Cut5a molecule, (S-S)1 that links cysteines 32 and 110, and (S-S)2 between cysteines 172 and 179 (Fig. 3A and 3B). The first disulphide bridge connects loop α1-β1 to loop α4-β3, while the

second one connects loop β5-α8 to helice α8. The three residues expected to function as a catalytic triad are Ser121, His189, and Asp176. Ser121 is located in a sharp turn between strand β5 and helice α5, called "nucleophilic elbow" and is typically present in all enzymes with α/β hydrolase fold. His189 is located on helice α9 and Asp176 is located on the loop β5-α8, which is stabilized by the (S-S)2 bond (Fig. 3B).

3.4 Comparison to other cutinase structures

The overall fold of *Fo*Cut5a is almost identical to previously determined cutinase structures. A search for structural homologues using the Dali server [50] revealed that *Fo*Cut5a is most similar to the *F. solani* cutinase, which was used to create a model for molecular replacement. The superposition of the two structures using secondary structure matching [51], gives a root-mean-square deviation (r.m.s.d) of C-alpha atoms of 0.48 Å between the two structures, indicating a very high similarity (Fig. 3A). The second closest structural homologue is *a Humicola insolens* cutinase (PDB ID: 4OYY, 54% sequence identity, and a r.m.s.d. of 0.8Å), followed by a *Glomerella cingulata* cutinase (PDB ID: 3DD5, 52% sequence identity, r.m.s.d. of 1Å).

By a visual inspection of the *Fo*Cut5a and *F. solani* superimposed structures, an almost identical overall fold is observed (Fig. 3A). Minor differences between the two structures can be seen in helix α3 and loop α3-α4, which are both situated on top of the active site cleft, as well as the region including residues 25 to 34, on the N-terminal part of the structure. A region close to helix α3 (residues 80-90) as well as loop α8-α9, which is located on top of the opposite side of the catalytic cleft, have been shown to exhibit a natural flexibility and the observed shift does not have any functional significance [52]. A more detailed analysis of the two structures, however, indicates that there are alterations in specific amino acids that could potentially affect the biochemical properties of the two highly homologous proteins. Specifically, the hydrophobic residues Ala62 and Phe63 in *F. solani* structure are replaced by two polar amino acids (Lys63 and Tyr64) in *Fo*Cut5a. These residues, which are located at the end of helix a2, form an additional hydrogen bond and an electrostatic interaction with Asp209, an amino acid located on helice α11, thus potentially increasing the overall thermal stability of *Fo*Cut5a (Fig 3D). In addition to that, *Fo*Cut5a has a glutamine instead of a glycine (Gly192) at position 193, which makes an additional hydrogen bond with the backbone oxygen of Leu190, bridging two

neighboring helices α9 and α10 (Fig. 3E). Nevertheless, the proline residue (Pro193) in *F. solani* structure that follows Gly192 could counterbalance the lack of the aforementioned hydrogen bond in terms of structural rigidity. On the other hand, Glu165, which is an alanine in case of *F. solani*, could be a source of instability for *Fo*Cut5a due to the repulsive force between the neighboring Glu165 and Asp166. Finally, Asp105 instead of Gln104 in *F. solani* structure, forms an close interaction with neighbouring Lys109, while Thr107 of *F. solani* makes an additional hydrogen bond to the backbone oxygen of Gln103 (Fig. 3C). Despite the high homology, *Fo*Cut5a seems slightly more thermostable than its *F. solani* counterpart, according to previously published experimental data for the latter (see paragraph 3.6 for details). Considering the interest for the industrial use and the lack of thermostability of most known cutinases (paragraph 3.6), the engineering of robust biocatalysts is of great importance. The aforementioned analysis could contribute to the identification of aminoacids potentially affecting enzyme stability for subsequent design of mutants with improved properties.

Previous studies have demonstrated the impact of differences in surface properties of closely related cutinase enzymes on PET hydrolysis [53]. Specifically, it has been shown that the physicochemical properties of residues outside the active site can considerably affect PET binding, hydrolysis products profile and overall efficiency. An analysis of the charge distribution on the surfaces of the *Fo*Cut5a and *F. solani* cutinases revealed two main regions of pronounced difference. The first one, indicated in green frames in Fig. 4, is a region that lies almost opposite to the active site and where *F. solani* displays significantly higher negative charge, comprising residues Asp21 and Asp33, which are Asn22 and Gly34 in case of *Fo*Cut5a. The other region, indicated in orange frames in Fig. 4, spans helix α1 and bears more positive charges in *Fo*Cut5a. This region consists of residues Ser54, Asn58 and Ala62 in *F. solani* and the corresponding residues in *Fo*Cut5a are Arg55, Lys59 and Lys63 (Fig. 4). Interestingly, both these regions can be related to ”region 1” of two *Thermobifida cellulosilytica* cutinases, Thc_Cut1 and Thc_Cut2, which has been shown to be crucial for PET hydrolysis [54]. In spite of their remarkable homology (93%), Thc_Cut1 is a much more efficient in hydrolysing PET than Thc_Cut2 is. Site-directed mutagenesis experiments have demonstrated that the charge and hydrophobicity of certain residues that belong to ”region 1” have significant impact on the functional properties of the two cutinases, and it was suggested that a neutral

potential in the region favours PET and 3PET degradation [54]. Verification of the functional significance of the aforementioned residues in *Fo*Cut5a structure requires additional mutation studies and activity measurements, and no definite conclusions can be drawn from the currently available data.

3.5 Kinetic studies of the recombinant cutinase

It has been shown that cutinases can hydrolyze a wide range of different substrates, including high molecular weight polyesters, emulsified or soluble triacylglycerols and synthetic *p*NPh esters. Among the three *p*NPh esters tested in this study, the recombinant enzyme showed the highest catalytic efficiency (k_{cat}/K_m) for the C_4-ester, followed by C_2- and C_{12}- esters. In specific, *Fo*Cut5a had a k_{cat} value of 111.9 ± 10 s^{-1} (Table 3) for the hydrolysis of butyrate ester (*p*NPhB) and a K_m of 0.7 ± 0.2 m*M*, which indicated a higher affinity in comparison to the other two esters. Such K_m value is comparable with the ones determined for cutinases originating from the fungi *T. harzanum* [42] and *Cryptococcus magnus* [55], and the bacteria *T. fusca* [56], *T. alba* [57] and *T. cellulosilytica* [58]. Similarly, activity and efficiency of *FoCut5a* (i.e. k_{cat} and k_{cat}/K_m constants) have similar values with cutinases already characterized [45, 46], except the one from *Pseudomonas cepacia*, which appears to be highly active (k_{cat} 22000 s^{-1}) [59].

3.6 Effect of temperature and pH on activity of *Fo*Cut5a

The optimum temperature for recombinantly expressed *Fo*Cut5a was determined to be 40 ^{o}C (Fig. 5A). A crude cutinase preparation from a wild-type *F. oxysporum* strain CBMAI 1274, exhibited optimal activity at 28 ^{o}C [60], while *cut1* from *F. solani* expressed in *P. pastoris* showed an optimum temperature of 40 ^{o}C [61]. Fungal cutinases that have been heterologously expressed in different expression systems exhibit optimal catalytic activity at temperatures varying from 25 ^{o}C (a cutinase from *G. cingulata* expressed in *E. coli* Origami B [62]) to 50 ^{o}C (a cutinase from *H. insolens* expressed in *P. pastoris*) [63]. On the other hand, bacterial thermophilic cutinases from *T. fusca* expressed in *E. coli* BL21, showed an optimal enzyme activity at 55-60 ^{o}C [45, 64].

Recombinantly expressed *Fo*Cut5a appeared to be more active at neutral-alkaline pHs. The optimum pH was found to be 8.0, while the enzyme was fairly active at pH

6.0, 7.0 and 9.0, showing respectively 57%, 62% and 44% of its optimum activity (Fig. 5B). Most cutinases, of both fungal (*F. solani* [61], *T. harzianum* [42], *C. magnus* [55]) and bacterial (*T. fusca* [45], *Pseudomonas cepacia* [65] and *Pseudomonas mendocina* [66]) origin, exhibit their catalytic optimum pH at 7.5-8.0. Some cutinases show their optimum activity in the acidic pH range 5.0-6.5, like the ones from *A. niger* [43] and *Botrytis cinerea* [67], or at even lower pH like the one from *T. terrestris* [38] (pH 4.0).

*Fo*Cut5a exhibited low temperature tolerance, being almost completely deactivated after 2 h incubation at 35 ^{o}C, while its intracellular counterpart was even more temperature sensitive, retaining only 37.6% of its activity after 1 h incubation at 20 ^{o}C. The different behavior between the cytoplasmic and periplasmic expression products might be explained by the oxidizing environment in periplasmic space, which favors the formation of the disulfide bonds necessary for the stabilization of the molecule [68]. Compared to its close homologue, originating from *F. solani*, it seems slightly more thermotolerant, as it retains 80% of its activity after 1h incubation at 30 ^{o}C, compared to 60% in the case of *F. solani* cutinase [28]. Improving the robustness of the latter has been the target of intensive research efforts, due to its potential as industrial biocatalyst [12, 49, 69]. *G. cingulata* cutinase, expressed in *E. coli* Origami B, exhibited a half-life of 30 min at 50 ^{o}C [62], while *T. terrestris* cutinase maintained its activity intact at 50 ^{o}C for 30 min [38]. On the other hand, a cutinase from *H. insolens* produced by *P. pastoris* X-33, lost only 10% of its initial catalytic activity after 48 h incubation at 50 ^{o}C [63], whereas thermophilic recombinant cutinases from the bacterial genus *Thermobifida* expressed in *E. coli*, are very stable in elevated temperatures, retaining more than 50% of their activity after 40 h at 60 ^{o}C [4] or after 80 h at 50 ^{o}C [64].

It has recently been reported that calcium ions can stimulate the activity and remarkably increase the thermostability of a cutinase from the thermophile *Saccharomonospora viridis* AHK190, named Cut190 [70]. The structure of Cut190 revealed that a calcium ion was coordinated by residues located close to the N-terminus of the protein. The observed enhancement could be explained by a rearrangement of some loops upon calcium binding and the formation of additional stabilizing interactions [71]. Even though *Fo*Cut5a shares very low sequence homology with Cut190, their overall fold is similar with an r.m.s.d. of 2.9 (calculated from the least squares superimposition of 150 structurally equivalent C-alpha atoms)

and a Z-score of 10.9 (Dali server). A structure-based sequence alignment between the two proteins did not show any conservation of the residues implicated in calcium binding. However, considering that in the case of *Fo*Cut5a structure 17 aminoacids in the N-terminus of the protein were not modelled due to undefined electron density, we examined the effect of high Ca^{2+} concentration on *Fo*Cut5a biochemical properties. The presence of 100 m*M* $CaCl_2$ resulted in an increase of *Fo*Cut5a activity by 20 %, but had no effect on its thermostability, contrary to what was found in the aforementioned study for Cut190 (data not shown).

3.7 Enzymatic hydrolysis of synthetic polyesters

Surface modification of PET fabrics aims at increasing their hydrophilicity and improving their properties [72]. In general, cutinases are capable of cleaving PET polymeric structures, however, the profile of hydrolysis products differs depending on the function and specificity of each cutinase. PET modification capability is not correlated to the enzymatic activity on different *p*-nitrophenyl esters, such as *p*NPhB that is commonly used for assaying cutinase activity [26]. Instead, two model substrates were used in the present study, 3PET and BHET, which can be hydrolyzed at different positions on their ester bonds and release different soluble fragments in the supernatant depending on the enzyme mode of action. As can be seen in Fig. 6A, *Fo*Cut5a hydrolyzes 3PET and the products involve TA, BHET and benzoic acid (BA) with concentrations of 0.19, 0.20 and 1.09 m*M*, respectively. The BHET product seems to be further hydrolyzed resulting in a BHET derivative, probably mono(2-hydroxyethyl)terephthalate (MHET) with a relative abundance of 46 %. This hypothesis was further proven by using BHET solely as substrate for *Fo*Cut5a, where MHET was released as main product, confirming the identity of the unknown peak (Fig. 6B). Previous studies have shown that cutinases from *T. fusca* and *F. solani* hydrolyze the model substrate 3PET releasing all possible fragments including TA, MHET, BHET, 2-hydroxyethyl-benzoate (HEB) and BA. Nevertheless, the almost total conversion of BHET to MHET and the significant release of HEB indicate a different mode of action for the two enzymes compared to *Fo*Cut5a [73].

The positive outcome of *Fo*Cut5a against PET model substrates was further confirmed by the successful release of TA or its derivatives (26 μ*M*) from PET

fabrics. The low amount of released TA equivalents is indicative of the anticipated mild surface hydrolysis, as reported in literature. For example, a commercial lipase from *Thermomyces lanuginosus* was found capable for the surface modification of semi-crystalline PET fibers by releasing similar amount of TA derivatives (~23 μ*M*) using an enzyme loading of 1.13 g protein per g polyester at 37 ^{o}C [74].

As far as PCL is concerned, the estimated weight loss after the enzymatic treatment is indicative of the ability of *Fo*Cut5a to degrade this kind of polyester in addition to PET. The weight loss of PCL granules after enzymatic hydrolysis was found to be 6%, which is lower compared to the weight loss after treatment with cutinases from *A. oryzae* and *F. solani*. It has been shown that at an enzyme load of 8.8 μ*M* of each of the two enzymes used for the hydrolysis of PCL films gave a weight loss of 87 and 30 %, respectively [28]. A lipase from *P. cepacia* (0.3 mg/mL) was also capable of hydrolyzing triethylbenzylammonium chloride (TEBAC) and SDS-containing PCL fibers reaching weight losses of 47 % and ~4 %, respectively [75]. Although *Fo*Cut5a capability to degrade PCL is experimentally proven by the reduced weight loss found, the different nature and amount of enzymes, as well as the shape and morphology of PCL used in literature prevent a reliable comparison and evaluation of the catalytic activity of the studied cutinase.

4 Conclusions

The present work is the first reported expression and crystal structure determination of a functional cutinase from the mesophilic fungus *F. oxysporum*. Expression in the bacterial periplasm at low temperature (16 ^{o}C) resulted in the highest yield of correctly folded, active enzyme. The structure of *Fo*Cut5a has a high similarity to already known cutinase structures. A detailed comparison between *Fo*Cut5a and the highly homologous *F. solani* cutinase structure, however, revealed dissimilarities in the electrostatic surface properties and aminoacid interactions that could influence the biochemical properties of the two enzymes. Finally, even though the natural role of cutinase in *F. oxysporum* plant pathogenicity requires further investigation, our findings show that *Fo*Cut5a can be used in biotechnological applications such as modification and degradation of PET based fabrics and other synthetic materials. Work is in progress for the optimization of the enzymatic surface modification of PET fabrics using *Fo*Cut5a, aiming at the hydrophilization of the final product without compromising the polymer bulk properties, such as strength.

Acknowledgements

The financial support of general Secretariat of Research and Technology (GSRT) of Greece-ESPA 2007–2013 is gratefully acknowledged (TEXT-ENZ project; 09SYN-81-601).

References

[1] A. Heredia, Biophysical and biochemical characteristics of cutin, a plant barrier biopolymer, Biochimica et biophysica acta, 1620 (2003) 1-7.
[2] R.E. Purdy, P.E. Kolattukudy, Hydrolysis of plant cuticle by plant pathogens. Properties of cutinase I, cutinase II, and a nonspecific esterase isolated from Fusarium solani pisi, Biochemistry, 14 (1975) 2832-2840.
[3] P. Skamnioti, R.F. Furlong, S.J. Gurr, Evolutionary history of the ancient cutinase family in five filamentous Ascomycetes reveals differential gene duplications and losses and in Magnaporthe grisea shows evidence of sub- and neo-functionalization, The New phytologist, 180 (2008) 711-721.
[4] S. Chen, X. Tong, R.W. Woodard, G. Du, J. Wu, J. Chen, Identification and characterization of bacterial cutinase, The Journal of biological chemistry, 283 (2008) 25854-25862.
[5] C. Martinez, P. De Geus, M. Lauwereys, G. Matthyssens, C. Cambillau, Fusarium solani cutinase is a lipolytic enzyme with a catalytic serine accessible to solvent, Nature, 356 (1992) 615-618.
[6] C. Martinez, A. Nicolas, H. van Tilbeurgh, M.P. Egloff, C. Cudrey, R. Verger, C. Cambillau, Cutinase, a lipolytic enzyme with a preformed oxyanion hole, Biochemistry, 33 (1994) 83-89.
[7] S. Chen, L. Su, J. Chen, J. Wu, Cutinase: characteristics, preparation, and application, Biotechnology advances, 31 (2013) 1754-1767.
[8] G.M. Guebitz, A. Cavaco-Paulo, Enzymes go big: surface hydrolysis and functionalization of synthetic polymers, Trends in biotechnology, 26 (2008) 32-38.
[9] Å.M. Ronkvist, W. Xie, W. Lu, R.A. Gross, Cutinase-Catalyzed Hydrolysis of Poly(ethylene terephthalate), Macromolecules, 42 (2009) 5128-5138.
[10] M. Alisch-Mark, A. Herrmann, W. Zimmermann, Increase of the hydrophilicity of polyethylene terephthalate fibres by hydrolases from Thermomonospora fusca and Fusarium solani f. sp. pisi, Biotechnology letters, 28 (2006) 681-685.
[11] M.A. Vertommen, V.A. Nierstrasz, M. Veer, M.M. Warmoeskerken, Enzymatic surface modification of poly(ethylene terephthalate), Journal of biotechnology, 120 (2005) 376-386.
[12] C.M. Carvalho, M.R. Aires-Barros, J.M. Cabral, Cutinase: from molecular level to bioprocess development, Biotechnol Bioeng, 66 (1999) 17-34.
[13] T. Nimchua, H. Punnapayak, W. Zimmermann, Comparison of the hydrolysis of polyethylene terephthalate fibers by a hydrolase from Fusarium oxysporum LCH I and Fusarium solani f. sp. pisi, Biotechnology journal, 2 (2007) 361-364.
[14] M. Moukouli, E. Topakas, P. Christakopoulos, Cloning, characterization and functional expression of an alkalitolerant type C feruloyl esterase from Fusarium oxysporum, Appl Microbiol Biotechnol, 79 (2008) 245-254.
[15] A. Steinle, P. Li, D.L. Morris, V. Groh, L.L. Lanier, R.K. Strong, T. Spies, Interactions of human NKG2D with its ligands MICA, MICB, and homologs of the mouse RAE-1 protein family, Immunogenetics, 53 (2001) 279-287.
[16] U.K. Laemmli, Cleavage of structural proteins during the assembly of the head of bacteriophage T4, Nature, 227 (1970) 680-685.
[17] C.M. Stoscheck, Quantitation of protein, Methods in enzymology, 182 (1990) 50-68.
[18] W. Kabsch, Xds, Acta crystallographica. Section D, Biological crystallography, 66 (2010) 125-132.
[19] A.J. McCoy, R.W. Grosse-Kunstleve, P.D. Adams, M.D. Winn, L.C. Storoni, R.J. Read, Phaser crystallographic software, Journal of applied crystallography, 40 (2007) 658-674.
[20] N. Stein, CHAINSAW: a program for mutating pdb files used as templates in molecular replacement, Journal of applied crystallography, 41 (2008) 641-643.
[21] S. Longhi, M. Czjzek, V. Lamzin, A. Nicolas, C. Cambillau, Atomic resolution (1.0 A) crystal structure of Fusarium solani cutinase: stereochemical analysis, Journal of molecular biology, 268 (1997) 779-799.

[22] P. Emsley, B. Lohkamp, W.G. Scott, K. Cowtan, Features and development of Coot, Acta crystallographica. Section D, Biological crystallography, 66 (2010) 486-501.
[23] G.N. Murshudov, A.A. Vagin, E.J. Dodson, Refinement of macromolecular structures by the maximum-likelihood method, Acta crystallographica. Section D, Biological crystallography, 53 (1997) 240-255.
[24] V.B. Chen, W.B. Arendall, 3rd, J.J. Headd, D.A. Keedy, R.M. Immormino, G.J. Kapral, L.W. Murray, J.S. Richardson, D.C. Richardson, MolProbity: all-atom structure validation for macromolecular crystallography, Acta crystallographica. Section D, Biological crystallography, 66 (2010) 12-21.
[25] E.F. Pettersen, T.D. Goddard, C.C. Huang, G.S. Couch, D.M. Greenblatt, E.C. Meng, T.E. Ferrin, UCSF Chimera--a visualization system for exploratory research and analysis, Journal of computational chemistry, 25 (2004) 1605-1612.
[26] S. Heumann, A. Eberl, H. Pobeheim, S. Liebminger, G. Fischer-Colbrie, E. Almansa, A. Cavaco-Paulo, G.M. Gubitz, New model substrates for enzymes hydrolysing polyethyleneterephthalate and polyamide fibres, Journal of biochemical and biophysical methods, 69 (2006) 89-99.
[27] M.Y. Yoon, J. Kellis, A.J. Poulose, Enzymatic modification of polyester, Aatcc Rev, 2 (2002) 33-36.
[28] Z. Liu, Y. Gosser, P.J. Baker, Y. Ravee, Z. Lu, G. Alemu, H. Li, G.L. Butterfoss, X.P. Kong, R. Gross, J.K. Montclare, Structural and functional studies of Aspergillus oryzae cutinase: enhanced thermostability and hydrolytic activity of synthetic ester and polyester degradation, Journal of the American Chemical Society, 131 (2009) 15711-15716.
[29] M.I.G. Roncero, C. Hera, M. Ruiz-Rubio, F.I.G. Maceira, M.P. Madrid, Z. Caracuel, F. Calero, J. Delgado-Jarana, R. Roldan-Rodriguez, A.L. Martinez-Rocha, C. Velasco, J. Roa, M. Martin-Urdiroz, D. Cordoba, A. Di Pietro, Fusarium as a model for studying virulence in soilborne plant pathogens, Physiol Mol Plant P, 62 (2003) 87-98.
[30] D. Li, T. Sirakova, L. Rogers, W.F. Ettinger, P.E. Kolattukudy, Regulation of constitutively expressed and induced cutinase genes by different zinc finger transcription factors in Fusarium solani f. sp. pisi (Nectria haematococca), The Journal of biological chemistry, 277 (2002) 7905-7912.
[31] A.L. Rocha, A. Di Pietro, C. Ruiz-Roldan, M.I. Roncero, Ctf1, a transcriptional activator of cutinase and lipase genes in Fusarium oxysporum is dispensable for virulence, Molecular plant pathology, 9 (2008) 293-304.
[32] B.L. Cantarel, P.M. Coutinho, C. Rancurel, T. Bernard, V. Lombard, B. Henrissat, The Carbohydrate-Active EnZymes database (CAZy): an expert resource for Glycogenomics, Nucleic Acids Res, 37 (2009) D233-238.
[33] S.F. Altschul, T.L. Madden, A.A. Schaffer, J. Zhang, Z. Zhang, W. Miller, D.J. Lipman, Gapped BLAST and PSI-BLAST: a new generation of protein database search programs, Nucleic acids research, 25 (1997) 3389-3402.
[34] W.F. Ettinger, S.K. Thukral, P.E. Kolattukudy, Structure of cutinase gene, cDNA, and the derived amino acid sequence from phytopathogenic fungi, Biochemistry, 26 (1987) 7883-7892.
[35] N. Blom, T. Sicheritz-Ponten, R. Gupta, S. Gammeltoft, S. Brunak, Prediction of post-translational glycosylation and phosphorylation of proteins from the amino acid sequence, Proteomics, 4 (2004) 1633-1649.
[36] S. Sulaiman, S. Yamato, E. Kanaya, J.J. Kim, Y. Koga, K. Takano, S. Kanaya, Isolation of a novel cutinase homolog with polyethylene terephthalate-degrading activity from leaf-branch compost by using a metagenomic approach, Applied and environmental microbiology, 78 (2012) 1556-1562.

[37] L. Su, R.W. Woodard, J. Chen, J. Wu, Extracellular location of Thermobifida fusca cutinase expressed in Escherichia coli BL21(DE3) without mediation of a signal peptide, Applied and environmental microbiology, 79 (2013) 4192-4198.
[38] S. Yang, H. Xu, Q. Yan, Y. Liu, P. Zhou, Z. Jiang, A low molecular mass cutinase of Thielavia terrestris efficiently hydrolyzes poly(esters), Journal of industrial microbiology & biotechnology, 40 (2013) 217-226.
[39] C.L. Soliday, W.H. Flurkey, T.W. Okita, P.E. Kolattukudy, Cloning and structure determination of cDNA for cutinase, an enzyme involved in fungal penetration of plants, Proceedings of the National Academy of Sciences of the United States of America, 81 (1984) 3939-3943.
[40] G.Y. Wang, T.J. Michailides, B.D. Hammock, Y.M. Lee, R.M. Bostock, Molecular cloning, characterization, and expression of a redox-responsive cutinase from Monilinia fructicola (Wint.) Honey, Fungal genetics and biology : FG & B, 35 (2002) 261-276.
[41] C.L. Soliday, P.E. Kolattukudy, Isolation and characterization of a cutinase from Fusarium roseum culmorum and its immunological comparison with cutinases from F. solani pisi, Archives of biochemistry and biophysics, 176 (1976) 334-343.
[42] M.B. Rubio, R.E. Cardoza, R. Hermosa, S. Gutierrez, E. Monte, Cloning and characterization of the Thcut1 gene encoding a cutinase of Trichoderma harzianum T34, Current genetics, 54 (2008) 301-312.
[43] A. Nyyssola, V. Pihlajaniemi, R. Jarvinen, S. Mikander, H. Kontkanen, K. Kruus, H. Kallio, J. Buchert, Screening of microbes for novel acidic cutinases and cloning and expression of an acidic cutinase from Aspergillus niger CBS 513.88, Enzyme Microb Technol, 52 (2013) 272-278.
[44] D. Castro-Ochoa, C. Pena-Montes, A. Gonzalez-Canto, A. Alva-Gasca, R. Esquivel-Bautista, A. Navarro-Ocana, A. Farres, ANCUT2, an extracellular cutinase from Aspergillus nidulans induced by olive oil, Applied biochemistry and biotechnology, 166 (2012) 1275-1290.
[45] K. Hegde, V.D. Veeranki, Production optimization and characterization of recombinant cutinases from Thermobifida fusca sp. NRRL B-8184, Applied biochemistry and biotechnology, 170 (2013) 654-675.
[46] E. Herrero Acero, D. Ribitsch, G. Steinkellner, K. Gruber, K. Greimel, I. Eiteljoerg, E. Trotscha, R. Wei, W. Zimmermann, M. Zinn, A. Cavaco-Paulo, G. Freddi, H. Schwab, G. Guebitz, Enzymatic Surface Hydrolysis of PET: Effect of Structural Diversity on Kinetic Properties of Cutinases from Thermobifida, Macromolecules, 44 (2011) 4632-4640.
[47] D. Ribitsch, E.H. Acero, K. Greimel, I. Eiteljoerg, E. Trotscha, G. Freddi, H. Schwab, G.M. Guebitz, Characterization of a new cutinase from Thermobifida alba for PET-surface hydrolysis, Biocatalysis and Biotransformation, 30 (2012) 2-9.
[48] Z. Chen, C.F. Franco, R.P. Baptista, J.M. Cabral, A.V. Coelho, C.J. Rodrigues, Jr., E.P. Melo, Purification and identification of cutinases from Colletotrichum kahawae and Colletotrichum gloeosporioides, Applied microbiology and biotechnology, 73 (2007) 1306-1313.
[49] E.P. Melo, R.P. Baptista, J.M.S. Cabral, Improving cutinase stability in aqueous solution and in reverse micelles by media engineering, J Mol Catal B-Enzym, 22 (2003) 299-306.
[50] L. Holm, P. Rosenstrom, Dali server: conservation mapping in 3D, Nucleic acids research, 38 (2010) W545-549.
[51] E. Krissinel, K. Henrick, Secondary-structure matching (SSM), a new tool for fast protein structure alignment in three dimensions, Acta crystallographica. Section D, Biological crystallography, 60 (2004) 2256-2268.
[52] S. Longhi, A. Nicolas, L. Creveld, M. Egmond, C.T. Verrips, J. de Vlieg, C. Martinez, C. Cambillau, Dynamics of Fusarium solani cutinase investigated through structural comparison among different crystal forms of its variants, Proteins, 26 (1996) 442-458.

[53] E.H. Acero, Ribitsch, D., Steinkellner, G., Gruber, K., Greimel, K., Eiteljoerg, I., Trotscha, Wei, R., Zimmermann, W., Zinn, M., Cavaco-Paulo, A., Freddi, G., Schwab, H., Guebitz, G., Enzymatic Surface Hydrolysis of PET: Effect of Structural Diversity on Kinetic Properties of Cutinases from Thermobifida, Macromolecules, 44 (2011) 4632-4640.
[54] E.H. Acero, D. Ribitsch, A. Dellacher, S. Zitzenbacher, A. Marold, G. Steinkellner, K. Gruber, H. Schwab, G.M. Guebitz, Surface Engineering of a Cutinase From Thermobifida Cellulosilytica for Improved Polyester Hydrolysis, Biotechnol Bioeng, 110 (2013) 2581-2590.
[55] K. Suzuki, H. Sakamoto, Y. Shinozaki, J. Tabata, T. Watanabe, A. Mochizuki, M. Koitabashi, T. Fujii, S. Tsushima, H.K. Kitamoto, Affinity purification and characterization of a biodegradable plastic-degrading enzyme from a yeast isolated from the larval midgut of a stag beetle, Aegus laevicollis, Applied microbiology and biotechnology, 97 (2013) 7679-7688.
[56] S. Chen, L. Su, S. Billig, W. Zimmermann, J. Chen, J. Wu, Biochemical characterization of the cutinases from Thermobifida fusca, Journal of Molecular Catalysis B: Enzymatic, 63 (2010) 121-127.
[57] D. Ribitsch, A.O. Yebra, S. Zitzenbacher, J. Wu, S. Nowitsch, G. Steinkellner, K. Greimel, A. Doliska, G. Oberdorfer, C.C. Gruber, K. Gruber, H. Schwab, K. Stana-Kleinschek, E.H. Acero, G.M. Guebitz, Fusion of binding domains to Thermobifida cellulosilytica cutinase to tune sorption characteristics and enhancing PET hydrolysis, Biomacromolecules, 14 (2013) 1769-1776.
[58] E. Herrero Acero, D. Ribitsch, A. Dellacher, S. Zitzenbacher, A. Marold, G. Steinkellner, K. Gruber, H. Schwab, G.M. Guebitz, Surface engineering of a cutinase from Thermobifida cellulosilytica for improved polyester hydrolysis, Biotechnology and bioengineering, 110 (2013) 2581-2590.
[59] K. Dutta, S. Sen, V.D. Veeranki, Production, characterization and applications of microbial cutinases, Process Biochemistry, 44 (2009) 127-134.
[60] P. Speranza, G. Alves Macedo, Biochemical characterization of highly organic solvent-tolerant cutinase from Fusarium oxysporum, Biocatalysis and Agricultural Biotechnology, 2 (2013) 372-376.
[61] M.A. Kwon, H.S. Kim, T.H. Yang, B.K. Song, J.K. Song, High-level expression and characterization of Fusarium solani cutinase in Pichia pastoris, Protein expression and purification, 68 (2009) 104-109.
[62] I.S. Chin, A.M. Abdul Murad, N.M. Mahadi, S. Nathan, F.D. Abu Bakar, Thermal stability engineering of Glomerella cingulata cutinase, Protein engineering, design & selection : PEDS, 26 (2013) 369-375.
[63] C. Kazenwadel, S. Eiben, S. Maurer, H. Beuttler, D. Wetzl, B. Hauer, K. Koschorreck, Thiol-functionalization of acrylic ester monomers catalyzed by immobilized Humicola insolens cutinase, Enzyme Microb Technol, 51 (2012) 9-15.
[64] L. Su, S. Chen, L. Yi, R.W. Woodard, J. Chen, J. Wu, Extracellular overexpression of recombinant Thermobifida fusca cutinase by alpha-hemolysin secretion system in E. coli BL21(DE3), Microbial cell factories, 11 (2012) 8.
[65] K. Dutta, H. Krishnamoorthy, V. Venkata Dasu, Novel cutinase from Pseudomonas cepacia NRRL B 2320: purification, characterization and identification of cutinase encoding genes, The Journal of general and applied microbiology, 59 (2013) 171-184.
[66] O. Degani, S. Gepstein, C.G. Dosoretz, Potential use of cutinase in enzymatic scouring of cotton fiber cuticle, Applied biochemistry and biotechnology, 102-103 (2002) 277-289.
[67] C.J. van der Vlugt-Bergmans, C.A. Wagemakers, J.A. van Kan, Cloning and expression of the cutinase A gene of Botrytis cinerea, Molecular plant-microbe interactions : MPMI, 10 (1997) 21-29.
[68] J.H. Choi, S.Y. Lee, Secretory and extracellular production of recombinant proteins using Escherichia coli, Applied microbiology and biotechnology, 64 (2004) 625-635.

[69] R.P. Baptista, S. Pedersen, G.J. Cabrita, D.E. Otzen, J.M. Cabral, E.P. Melo, Thermodynamics and mechanism of cutinase stabilization by trehalose, Biopolymers, 89 (2008) 538-547.
[70] F. Kawai, M. Oda, T. Tamashiro, T. Waku, N. Tanaka, M. Yamamoto, H. Mizushima, T. Miyakawa, M. Tanokura, A novel Ca(2)(+)-activated, thermostabilized polyesterase capable of hydrolyzing polyethylene terephthalate from Saccharomonospora viridis AHK190, Applied microbiology and biotechnology, 98 (2014) 10053-10064.
[71] T. Miyakawa, H. Mizushima, J. Ohtsuka, M. Oda, F. Kawai, M. Tanokura, Structural basis for the Ca-enhanced thermostability and activity of PET-degrading cutinase-like enzyme from Saccharomonospora viridis AHK190, Applied microbiology and biotechnology, (2014).
[72] G.M. Gübitz, A.C. Paulo, New substrates for reliable enzymes: enzymatic modification of polymers, Current Opinion in Biotechnology, 14 (2003) 577-582.
[73] A. Eberl, S. Heumann, T. Bruckner, R. Araujo, A. Cavaco-Paulo, F. Kaufmann, W. Kroutil, G.M. Guebitz, Enzymatic surface hydrolysis of poly(ethylene terephthalate) and bis(benzoyloxyethyl) terephthalate by lipase and cutinase in the presence of surface active molecules, J Biotechnol, 143 (2009) 207-212.
[74] T. Brueckner, A. Eberl, S. Heumann, M. Rabe, G.M. Guebitz, Enzymatic and chemical hydrolysis of poly(ethylene terephthalate) fabrics, J Polym Sci Pol Chem, 46 (2008) 6435-6443.
[75] J. Zeng, X. Chen, Q. Liang, X. Xu, X. Jing, Enzymatic degradation of poly(L-lactide) and poly(epsilon-caprolactone) electrospun fibers, Macromolecular bioscience, 4 (2004) 1118-1125.
[76] S. Longhi, M. Mannesse, H.M. Verheij, G.H. De Haas, M. Egmond, E. Knoops-Mouthuy, C. Cambillau, Crystal structure of cutinase covalently inhibited by a triglyceride analogue, Protein science : a publication of the Protein Society, 6 (1997) 275-286.

Figure 1. SDS-PAGE (A) and IEF (B) of *Fo*Cut5a. (A) Lanes: 1, *E. coli* BL21 crude intracellular cell fraction; 2, IMAC flow through; 3, Pink prestained protein marker (Nippon Genetics Europe); 4, purified *Fo*Cut5a. (B) Lanes: 1 and 4, standard protein markers with pI range 3.5-9.3; 2 and 3, purified *Fo*Cut5a.

Figure 2 Pairwise amino acid sequence alignment of *Fo*Cut5a and *F. solani pisi* cutinase (indicated as FsCut1). The residues not present in the crystallographic structures are indicated in a blue frame. The secondary structure assignment refers to *Fo*Cut5a. β-strands are shown as blue arrows and α-helices as purple cylinders. Black stars indicate the catalytic triad residues of both enzymes. Identical residues are shown in white on a red background and similar residues are shown in red on a white background.

Figure 3 A: Superimposed *Fo*Cut5A (in green) and *F. solani* cutinase (in grey) crystal structures, showing the almost identical fold. The active site residues and the two disulfide bridges of *Fo*Cut5A are shown in stick representation. A close-up view of the active site is shown in (B). The yellow frames indicate the regions that are shown zoomed-in in C, D and E., where *Fo*Cut5a residues are labeled in green and *F. solani* residues in grey. The distances (in Å) of the bonds are presented as black dashed lines.

Figure 4. Coulombic surface representation of *F. solani* (left) and *F. oxysporum* (right) where red colour represents negative and blue colour represents positive charge. Regions with different electrostatic potential are highlighted in orange and green frames, and the residues belonging to these regions are indicated for each enzyme. A triglyceride analogue (derived from a crystallographic complex of *F. solani* cutinase with PDB ID: 1OXM [76]) is shown in sticks (magenta), indicating the location of the active site is in both enzymes.

Figure 5. Effect of temperature (A) and pH (B) on the activity of the recombinant *Fo*Cut5.

Figure 6. A. HPLC chromatogram of (A) 3PET and (B) BHET hydrolysis catalyzed by a *Fo*Cut5a after 18 h of incubation in 100 mM Tris-HCl buffer pH 7 at 30 ^{o}C. The hydrolysis reaction is represented by a solid line, while dotted line represents the control reaction without enzyme added to the reaction mixture.

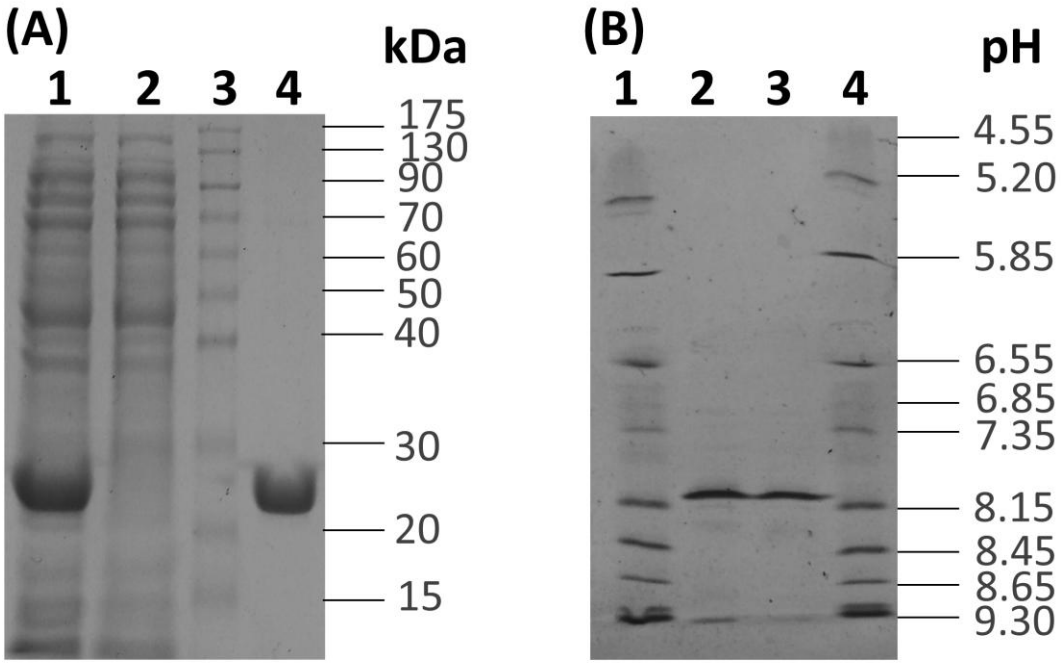

Figure 1

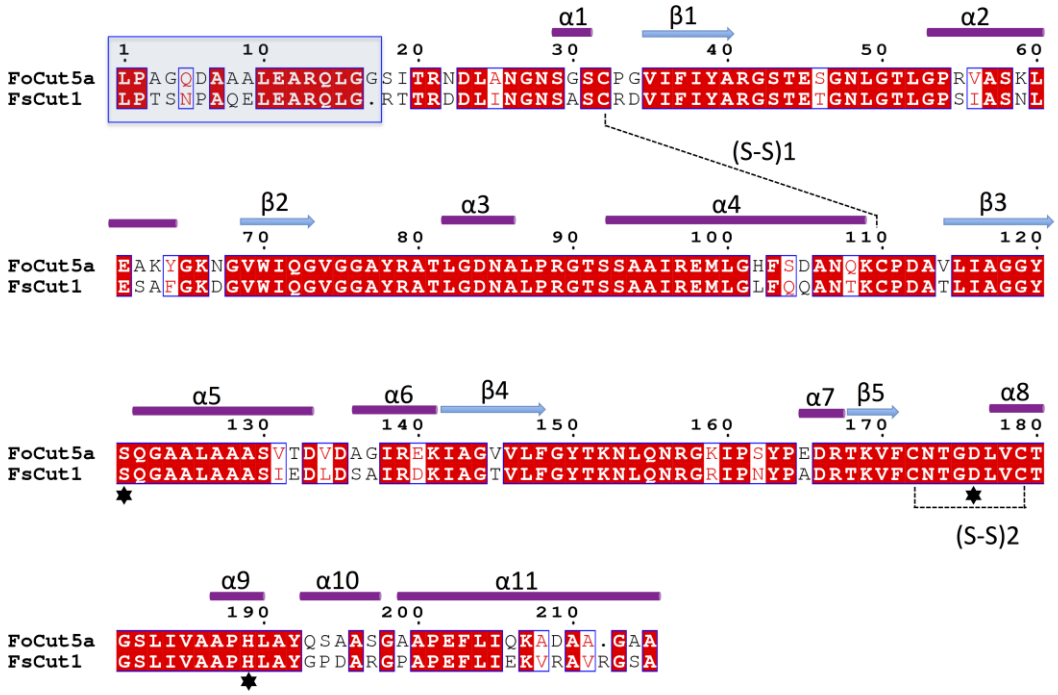

Figure 2

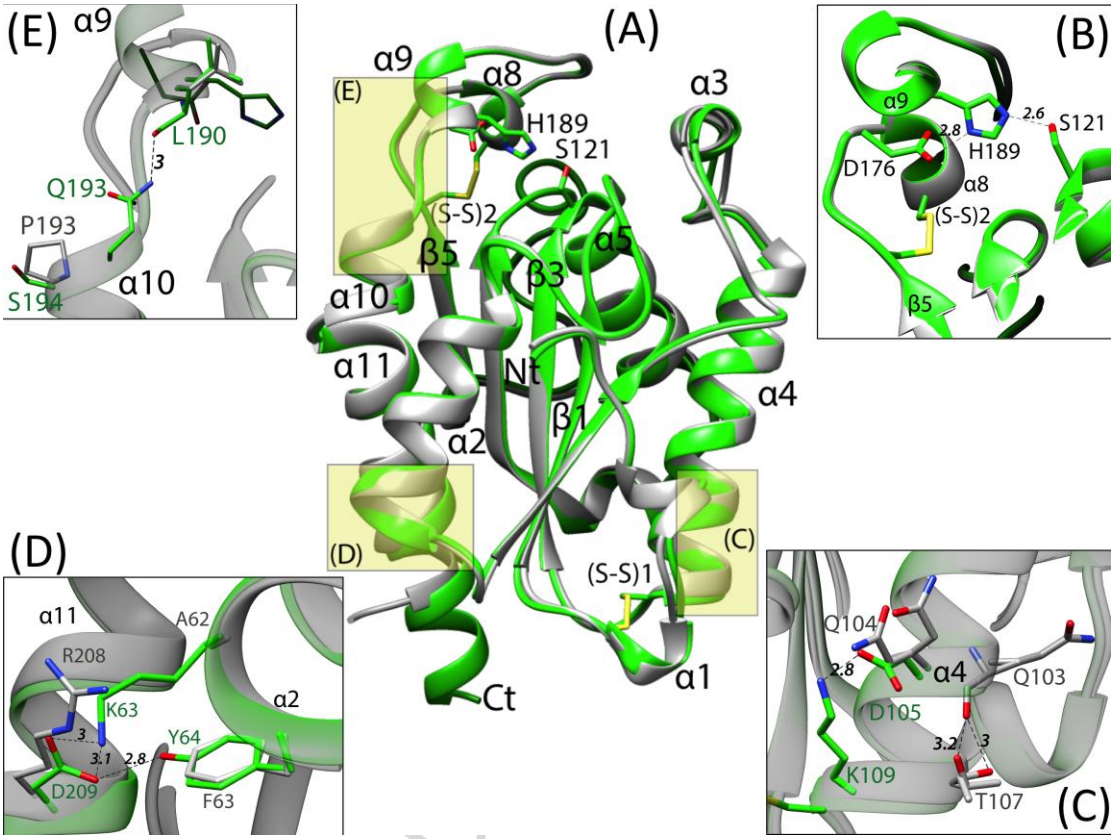

Figure 3

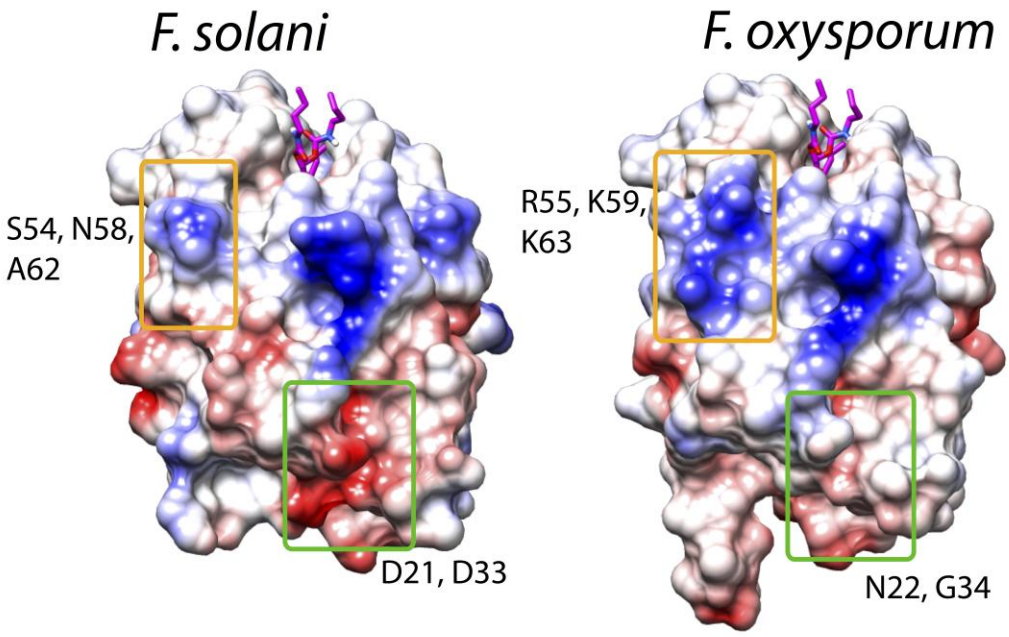

Figure 4

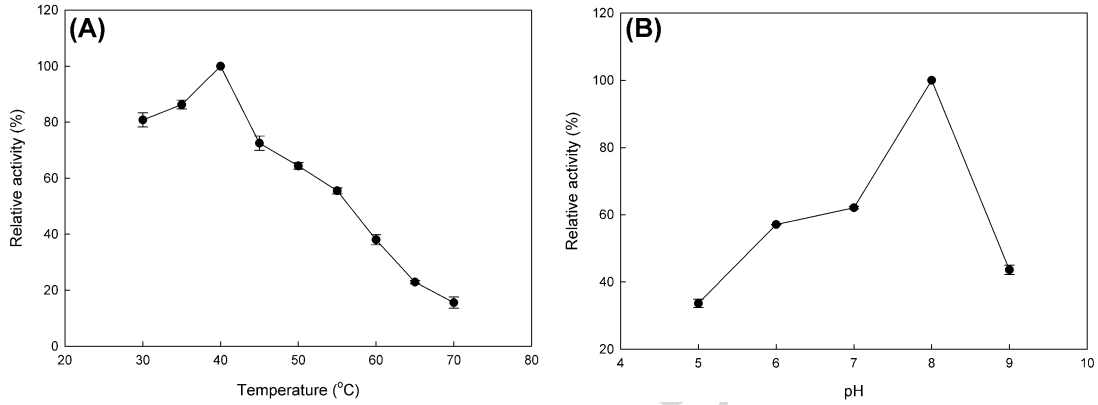

Figure 5

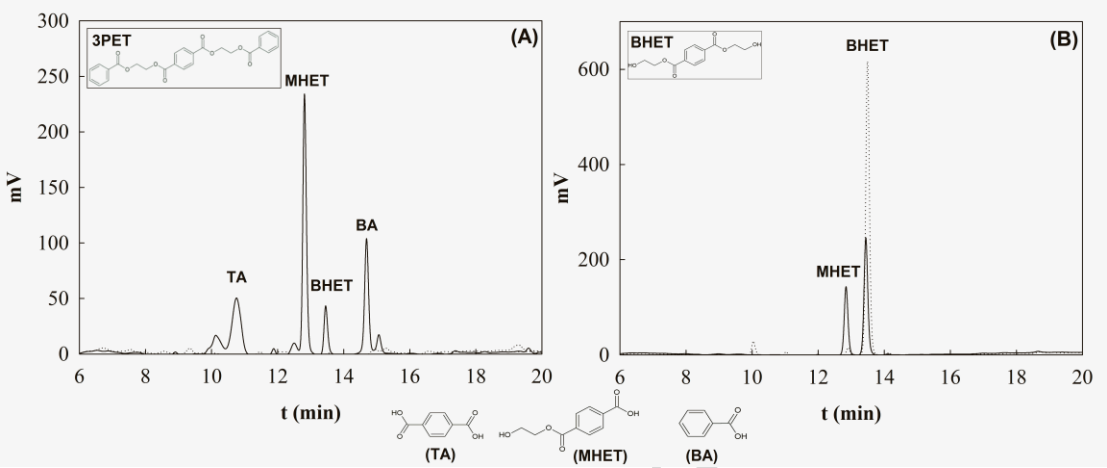

Figure 6

Table 1

Name, oligonucleotide sequence and molecular length (measured in number of nucleotides nt) of the primers synthesized for the cloning of *cut5a* gene.

Name	Oligonucleotide sequence (5'→3') [a]	Length (nt)
*Fo*Cut5a_F	GCCATATGCTTCCCGCTGGTCAGGATGC	28
*Fo*Cut5a_R	CGGCGGCCGCTCCAGCAGCATCAGCCTTCTG	31
*Fo*Cut5a_eF	GGAACTCTCGGTCCCCGCG	19
*Fo*Cut5a_eR	GGGACCGAGAGTTCCAAGGTTGCCAGATTCAGT GGAGC	38
*Fo*Cut5a_pelBF	GCCCATGGATCTTCCCGCTGGTCAGGATGCCG	32

[a] The restriction sites introduced in the primer sequences are underlined (*Nde*I: CATATG, *Not*I: GCGGCCGC, *Nco*I: CCATGG).

Table 2. Diffraction data and refinement statistics for *Fo*Cut5a structure

Data collection and Refinement Statistics	
Data collection	
Beamline	ID23-2 (ESRF)
Wavelength (Å)	0.8726
Space group	$P2_12_12_1$
Cell dimensions (a, b, c) (Å)	a=35.9, b=60.1, c=241.9
No. of molecules per asymmetric unit	3
Resolution (Å) (outermost shell)	48.4-1.9 (1.94-1.9)
No. of observations	366032 (22725)[a]
No. of unique reflections	42540 (2679)[a]
Completeness (%)	99.8 (100)[a]
[b] R_{merge} (%)	23.3 (127) [a]
[c] R_{pim} (%)	8.9 (49.1) [a]
Mean((I/sd(I))	7.5 (1.5) [a]
[d] $CC_{1/2}$	99.8 (59.7) [a]
Multiplicity	8.6 (8.5) [a]
Wilson *B* value (Å^2)	6.7
Refinement statistics	
R_{work}/R_{free} (%)	18.1/22.4
R.m.s.d., bond lengths (Å)	0.008
R.m.s.d., bond angles (^{o})	1.212
Reflections (work)	40392 (2913) [a]
Reflections (test)	2067 (164) [a]
No. of protein atoms	4246
No. of solvent molecules	468
No. of MPD molecules	6
Average B-values (Å^2)	
All proteins	18.54
Water molecules	28.95
MPD molecules	39.10
[e]Ramachandran statistics (%)	
Favored	97.48
Outliers	0
Rotamers outliers	0.24%
PDB ID	5AJH

[a] Numbers in parentheses refer to the highest resolution shell (1.94-1.9 for diffraction data and 1.95-1.9 for refinement), [b] $R_{merge} = \Sigma_{hkl} \Sigma_i | I_i(hkl) - \langle I(hkl) \rangle | / \Sigma_{hkl} \Sigma_i I_i(hkl)$, [c] $R_{pim} = \Sigma_{hkl} (N\text{-}1)^{-1/2} \Sigma_i | I_i(hkl) - \langle I(hkl) \rangle | / \Sigma_{hkl} \Sigma_i I_i(hkl)$, [d] CC1/2 is the correlation coefficient between two random half datasets, [e] Calculated using Molprobity (http://molprobity.biochem.duke.edu/)

Table 3

Substrate specificity for the hydrolysis of different *p*-nitrophenyl esters of aliphatic acids. Kinetic constants (K_m and k_{cat}) were determined using GraphPad Prism 5 that gives an estimate of the standard error (numbers in parentheses). K_m is expressed as mM and k_{cat} as sec^{-1}.

	K_m	k_{cat}	k_{cat}/K_m
p-NPhA	5.4 (1.5)	121 (15.5)	22.5 (6.7)
p-NPhB	0.7 (0.2)	111.9 (10)	152.5 (37.5)
p-NPhL	2.1 (0.4)	8.3 (1.4)	3.9 (1.1)

Highlights

- A cutinase from *F. oxysporum* was functionally expressed in the periplasm of *E. coli*
- *Fo*Cut5a X-ray structure was determined to 1.9Å resolution
- The cutinase was active on a variety of synthetic esters and polyester analogues
- *Fo*Cut5a could be used for the surface modification of PET synthetic polymers